



Published in final edited form as:

Cytoskeleton (Hoboken). 2013 January ; 70(1): 24–31. doi:10.1002/cm.21088.

Microtubule modifications and stability are altered by cilia perturbation and in cystic kidney disease

Nicolas F. Berbari^{1,†}, Neeraj Sharma^{1,†}, Erik B. Malarkey¹, Jay N. Pieczynski¹, Ravindra Boddu², Jacek Gaertig³, Lisa Guay-Woodford^{2,4}, and Bradley K. Yoder^{1,*}

¹Department of Cell, Developmental and Integrative Biology, University of Alabama at Birmingham, Birmingham, AL 35294 USA

²Department of Genetics, University of Alabama at Birmingham, Birmingham, AL 35294

³Department of Cell Biology, University of Georgia, Athens, GA 30602

⁴The George Washington University, Children's National Medical Center, 111 Michigan Ave NW, Washington, DC 20010

Summary

Disruption of the primary cilium is associated with a growing number of human diseases collectively termed *ciliopathies*. Ciliopathies present with a broad range of clinical features consistent with the near ubiquitous nature of the organelle and its role in diverse signaling pathways throughout development and adult homeostasis. The clinical features associated with cilia dysfunction can include such phenotypes as polycystic kidneys, skeletal abnormalities, blindness, anosmia, and obesity. Although the clinical relevance of the primary cilium is evident, the effects that cilia dysfunction has on the cell and how this contributes to disease remains poorly understood. Here, we show that loss of ciliogenesis genes such as *Ift88* and *Kif3a* lead to increases in post-translational modifications on cytosolic microtubules. This effect was observed in cilia mutant kidney cells grown in vitro and in vivo in cystic kidneys. The hyper-acetylation of microtubules resulting from cilia loss is associated with both altered microtubule stability and increased α -tubulin acetyl-transferase activity. Intriguingly, the effect on microtubules was also evident in renal samples from patients with autosomal recessive polycystic kidneys. These findings indicate that altered microtubule post-translational modifications may influence some of the phenotypes observed in ciliopathies.

Keywords

cilia; tubulin; acetylation; microtubules; Polycystic Kidney Disease

Introduction

Despite their involvement in complex cellular behaviors such as cell shape, migration, cytokinesis, and intracellular transport, at their core, microtubules consist of relatively simple polymerized α and β -tubulin heterodimers. Although microtubules form the structural backbone of stable and complex cellular features such as the cilium and centrosomes, they can also undergo depolymerization and polymerization to regulate processes that require rapid responses. The ability to continually add or subtract tubulin to

*Corresponding Author: Bradley K. Yoder, Ph.D., Department of Cell Biology, 1918 University Blvd., Birmingham, AL 35294, Phone: (205) 934-0995, FAX: (205) 934-0990, byoder@uab.edu.

[†]Authors contributed equally to this work

the same end of a microtubule filament is referred to as dynamic instability (Mitchison and Kirschner 1984). Interestingly, microtubule structures with a slow turnover such as those forming the centrosome and ciliary axoneme possess tubulin that is highly enriched in post-translational modifications (PTMs) such as acetylation and polyglutamylation. Data suggest that PTMs contribute to regulation of microtubule properties, in particular the ability to interact with motors and depolymerizing factors (reviewed in Janke and Bulinski 2011); however, little is known about how microtubule PTM is regulated in vivo.

The primary cilium is a small cellular appendage found on most eukaryotic cells. The cilium's backbone, the axoneme, contains microtubules routinely associated with PTMs such as acetylation (L'Hernault and Rosenbaum 1985; Piperno and Fuller 1985). While it is clear that the cilium and the cellular cytoskeleton are connected through the basal body/centrosome, it is currently unknown whether the loss of cilia or its functions can influence the cytoskeletal architecture and thus alter cellular behaviors.

The tight physical association between the cilium and cytoskeleton raises the possibility of reciprocal communications between these two structures and that defects in one may alter the other. Indeed, recent work by Loktev et al. showed that knockdown of the ciliopathy associated protein BBIP10 inhibits the assembly of primary cilia in hTPE1 cells and decreases the levels of acetylation on cytoplasmic microtubules (Loktev et al. 2008). Conversely, other studies have indicated that cilia defects result in hyper-acetylation of cytosolic microtubules (Berbari et al. 2011). The mechanistic basis for these differences is unknown. Moreover, we demonstrated previously that subtle increases in the level of soluble tubulin resulting from treatment of cells with low nocodazole or colchicine concentrations induces cilia elongation and that this effect can be blocked by pretreatment with Taxol (Sharma et al. 2011). These results suggest there is an intimate connection between the cytosolic microtubule and actin networks that influence cilia assembly, and that the cilium can also affect the cytoskeleton. Understanding the relationship between cilia and cellular cytoskeletal regulation could provide important insights into the pathogenesis of rare ciliopathies and also into some common clinical features associated with these disorders.

Materials and Methods

Generation of kidney epithelial cell lines

Immortalized renal cell lines with a conditional allele of *Kif3a*^{tm2Gsn} (hereafter called *Kif3a*^{fl/fl}) and *Ift88*^{tm1Bky} (hereafter called IFT88^{fl/fl}) were generated from mice carrying both the SV40 ImmortoMouseTM transgene and the ubiquitously expressed tamoxifen inducible CAGG-cre/*Esr1/5Amc/J* (hereafter called CAGGCre^{ER}) as previously described (Yoder et al. 2002). Animals were maintained in AAALAC accredited facilities in accordance with IACUC regulations at the University of Alabama at Birmingham.

Cell Culture

Collecting duct cell lines and IMCD-3 cells (ATCC, Manassas, VA USA) were cultured as previously described (Berbari et al. 2008a; Sharma et al. 2011).

Immunofluorescence and Immunoblotting

For immunofluorescence, cells were fixed for preservation of cytoskeletal structures (Bell and Safiejko-Mrocicka 1995). Samples were processed for immunofluorescence and immunoblotting as previously described (Berbari et al. 2008b; Sharma et al. 2011). The primary antibodies were used and diluted as follows: anti-acetylated α -tubulin (T7451) 1:1000, anti- β -tubulin (T5201) 1:1000, anti- γ -tubulin (T6557 and T3559) 1:2000, anti-actin (A2066) 1:1000 (Sigma-Aldrich) anti- α -tubulin (ab18251) 1:1000, anti-HDAC6 (ab12173)

1:500 (Abcam, Cambridgeshire, UK), rabbit anti-IFT88 polyclonal 1:1000 (Haycraft et al. 2005), anti-Arl13b, 1:1500, anti-polyglutamylated tubulin 1:1000, and FITC conjugated anti-BrdU (A21303) 1:500 (Invitrogen, Carlsbad CA, USA). Secondary antibodies included: Alexa Fluor-546 and -488 conjugated goat anti-mouse IgG (A11003, A11001) and Alexa Fluor-546, -488, -647 (A10040, A21206, and A21244) conjugated donkey anti-rabbit IgG (Invitrogen). Nuclei were visualized by Hoechst 33342 (Invitrogen).

Image acquisition and analysis

Fluorescence images were captured on a Perkin Elmer ERS 6FE spinning disk confocal microscope equipped with lasers and filter sets for GFP, TRITC, Cy5 and DAPI fluorescence. Images were analyzed using Volocity 5.3 software (Perkin Elmer, Shelton, CT USA) to count cilia positive cells using its detect objects algorithm on Arl13b staining, to count total cells by detecting Hoechst stained nuclei and to quantify total tubulin fluorescence per cell. ImageJ 1.45 (National Institutes of Health, Bethesda, MD USA) was used to measure microtubule density using β -tubulin fluorescence in non-nuclear regions of the cells in background subtracted images as previously described (Sharma et al. 2007).

Proliferation analysis

Proliferation was analyzed using a BrdU labeling reagent at 1:100 (00–0103; Invitrogen) on cells at 30–40 % confluence. At 2 and 4 hours, cells were processed for immunofluorescence. Antigen retrieval was done using 2 M HCl (at 37 °C for 20 min) before FITC conjugated anti-BrdU antibody incubation. Proliferative indices (Total # BrdU positive nuclei/Total # Hoechst nuclei) were determined using 25 random images (40X magnification).

Microtubule depolymerization assays

Once 80–90% confluent, cells were incubated in increasing concentrations of nocodazole or DMSO for 2 hours. Cells were washed with PBS, fixed, and stained for immunofluorescence. For cold resistance experiments, cells were incubated at 4°C for 90 minutes.

For nocodazole and Taxol viability measurements, approximately 1000 cells were seeded into each of three replicate wells of 24-well dish containing collecting tubule media with increasing drug concentrations for 10 days. Surviving cells were stained by 0.5% methylene blue solution. To obtain quantitative data, dye was eluted in 500 μ l of 1% SDS and absorbance was read at 630 nm (Wang et al. 2004).

Microtubule polymerization and in vitro tubulin acetylation assay

Purification of total tubulin from the MEC17-KO strain of *T. thermophila* were generated and polymerized as described (Akella et al. 2010). Total cell extracts were prepared in lysis buffer (137 mM NaCl, 20 mM Tris-HCl, 1 % Triton X-100 and 10 % glycerol) on ice. Lysate was passed through syringe 2–3 times and incubated on ice for 45 min. The acetylation assays were performed at 28°C in the acetylation buffer in a 30 μ l reaction mixture that included 125ng/ μ l of polymerized Tetrahymena MEC17-KO tubulin, 1 μ g of cell extract, and 0.3 μ l of 1 mM Acetyl CoA. The reactions were stopped by 4X SDS sample buffer followed by heating at 96°C for 5 min after 5, 15 and 30 minutes. Proteins were separated on 12% SDS-gel and transferred onto nitrocellulose membrane and processed with antibodies as discussed above.

Induction of renal cyst formation in IFT88 conditional mutant mice

Induction of renal cysts in CAGGCreER; IFT88^{fl/fl} mice was performed as previously described (Davenport et al. 2007).

Human Cystic Kidney Samples

ARPKD samples were obtained through the “Analysis of Molecular Determinants in the Development of Polycystic Kidney Disease” protocol approved by the UAB Institutional Review Board. The first sample (148) was obtained post-mortem from a 2 month old male. The second sample (287) was obtained via nephrectomy in 11 day old female. Diagnosis was based on clinical findings and gross pathologic examination. A non-ARPKD kidney sample was obtained from a male neonate born at 36-week gestational age who died in the perinatal period due to ischemia. Samples were stored at -80°C prior to protein isolation for Western blotting. Western blot analysis was performed on the two independent patients and controls. Similar results were obtained with both samples and the result for patient 287 is shown in figure 4D.

Results and Discussion

To more directly assess possible connections between cilia and the cytoskeleton, we generated immortalized renal collecting duct cell lines in which cilia could be conditionally ablated. This was accomplished using a tamoxifen inducible cre recombinase and loxp flanked conditional alleles for either the IFT kinesin subunit *Kif3a* (hereafter called Kif3a^{fl/fl}). After treating cells with tamoxifen, loss of Ift88/Kif3a and presence or absence of cilia was assessed by western blot analysis and by immunostaining with the cilia marker Arl-13b (Fig. 1A, B, C). After 2–3 weeks in tamoxifen supplemented medium fewer than 15% of the cells possess a cilium. Surprisingly, we found that cilia on confluent cells were relatively stable and persisted for 6–7 days after the protein was absent (data not shown).

To assess whether cilia loss affected the PTM signature of the microtubule cytoskeleton, the cells were labeled with anti-acetyl α -tubulin, anti-polyglutamylation, and anti- α -tubulin antibodies. In cilia mutant cells there was an increase in levels of α -tubulin acetylation compared to controls (Figs 1C, D, and 3B). Western blot and immunofluorescence analysis indicate no major difference in levels of α -tubulin protein that could account for the increase in acetylation (Fig 1C and D). This difference between ciliated and nonciliated cells was not observed for glutamylated tubulin (Fig 1E). Although tamoxifen was not present in the medium of cells analyzed above, to exclude the possibility that tamoxifen treatment itself could alter tubulin PTM signature, PTM of tubulin was analyzed in IMCD3 cells treated with tamoxifen and no overt changes were observed. (Fig S1).

Interestingly, while our studies were ongoing, Blitzer *et al.* reported that corneal endothelial cells from *ift88^{orpk}* mice or normal corneal endothelial cells undergoing knockdown of IFT88 *in vivo* display greatly increased levels of cytosolic acetylated microtubules. The authors propose a role for the cilium in the cellular remodeling and cytoskeletal changes that occur during development and in tissue repair. It is possible the cilium is regulating similar effects in the context of the kidney during injury or response to cyst formation (Blitzer et al. 2011).

Several possibilities could lead to increases in cell body microtubule PTMs associated with cilia loss, such as altered cell proliferation rates, overall microtubule stability changes, or altered enzyme activity responsible for regulating microtubule PTMs. Changes caused by proliferation seem unlikely since proliferation rates were similar in ciliated and nonciliated cells (Fig S2).

Cilia loss alters the stability of cytoplasmic microtubules

The observation that some PTMs are increased in cilia mutants suggests that microtubule stability is enhanced (Khawaja et al. 1988; Webster and Borisy 1989). To assess whether microtubule stability is altered in cilia mutants, we analyzed cellular responses to microtubule stabilizing and destabilizing agents. Previous studies demonstrated that cells with defects in microtubule stability or dynamics exhibit altered sensitivity to further stabilization or destabilization (Ganguly and Cabral 2011; Goncalves et al. 2001; Goold et al. 1999). We treated *Kif3a* mutant and control cells with varying concentrations of the microtubule destabilizing agent, nocodazole and analyzed subsequent microtubule polymerization and cell survival. Under these conditions similar levels of polymerized microtubules and cell survival were observed for both control and cilia mutant cells (Fig. 2A, C). In contrast, cold sensitivity assays revealed that the microtubules in the mutants do not depolymerize as observed in the control cells supporting an increase in microtubule stability in the mutants (Fig. 2B). In contrast to results obtained with the depolymerizing agent, nocodazole, when microtubule stability was increased with Taxol there was a decrease in viability and a marked increase in Taxol sensitivity in cilia mutant cells (Fig. 2C), further indicating that cytosolic microtubules are more stable in the absence of the cilium.

Although the mechanism of cold induced depolymerization is currently poorly understood, a difference in cold and drug induced MT depolymerizing treatments has been reported previously in MDCK cells in a study by Quinones et al (Quinones et al. 2011). These authors identified subpopulations of microtubules with different combinations of PTM that change as cells undergo polarization. The findings indicate that regulation of PTMs on different microtubule populations in the cell is likely complex and change under altered differentiation conditions. These microtubules with distinct collections of PTMs appear to have different properties that feasibly convey diverse functionality to the microtubule network. In fact, different PTM on MT have been proposed as “navigation” cues for microtubule motor proteins to regulate protein transport and cell migration among other cellular activities (Hammond et al. 2010; Konishi and Setou 2009; Quinones et al. 2011).

Cilia loss leads to changes in tubulin modifying enzyme activity

Recently, the enzyme responsible for α -tubulin acetylation on lysine 40 was identified as α -TAT1/MEC-17 (Akella et al. 2010; Shida et al. 2010). Disruption of α -TAT1/Mec17 in mammalian cells and in *Tetrahymena thermophila* resulted in loss of α -tubulin K40 acetylation (Akella et al. 2010; Shida et al. 2010). While the absence of α -TAT1/MEC-17 did not affect cilia in *Tetrahymena* (Akella et al. 2010), in mammalian cells an siRNA knockdown of α -TAT1/MEC-17 led to a delay in ciliation in confluent cells (Shida et al. 2010). Interestingly, *Tetrahymena* MEC-17 knockout cells are hyper-resistant to Taxol but are sensitive to a microtubule depolymerizing agent such as oryzalin (Akella et al. 2010). These data indicate that in the absence of tubulin acetylation by MEC-17, the microtubules are more labile.

Based on the above data, we hypothesize that hyper-acetylation of cytosolic microtubules may be caused by enhanced acetyltransferase activity possibly by α -TAT1/MEC17. To test this possibility, we performed an in vitro acetylation assay using protein extracts prepared from cilia mutant and control cells incubated with purified tubulin obtained from *Tetrahymena* MEC-17 knockout cells (Akella et al. 2010). In agreement with an increase in tubulin acetylation activity, protein extracts from *Kif3a* mutant cells displayed an increased ability to acetylate mec17 KO polymerized microtubules compared to that observed with control extracts throughout the time course (Fig 3A).

To assess whether the changes in acetylated tubulin observed in cilia mutants could also be due to an inability to de-acetylate the microtubule, we analyzed expression and localization of histone deacetylase 6 (HDAC6), a key enzyme involved in regulating α -tubulin acetylation and microtubule dynamics (Hubbert et al. 2002; Zhang et al. 2003; Zilberman et al. 2009). In cilia mutants there is an increase in HDAC6 expression levels on immunofluorescence and Western blot analysis but no obvious change in the spatial distribution (Fig 3B, C, and D).

To assess whether activity of HDAC6 is also altered in cilia mutants, cell extracts were incubated with the HDAC6 inhibitor tubacin or related inactive compound niltubacin prior to addition of *Tetrahymena* microtubules. Addition of tubacin to cilia mutant extracts (+ Tamox.) results in nearly a two fold increase in levels of acetylated tubulin (Fig 3E, 0.53 to 1.0) compared to the same sample treated with niltubacin. In contrast, an increase in acetylated tubulin levels was not observed when ciliated extracts were treated with tubacin (Fig 3E, 0.13 to 0.07). The cause for the increase in HDAC6 activity is not known but could be related the increased acetyl transferase activity and the increased levels of acetylated tubulin in these cells.

In vivo models of cilia loss also display altered PTMs

We next assessed whether similar changes in microtubule PTMs occur in response to loss of cilia in vivo. This was done in *Iff88* conditional mutant kidney samples by Western analysis and by immunofluorescence in kidney sections (Fig. 4). Cilia extending from the basal body were readily detected in control animals but not in mutants (Fig. 4A). Similar to what we observed in cell culture, there was a marked increase in the level of acetylated α -tubulin without overt changes in the level of total α -tubulin in cilia mutants on Western blot analysis (Fig 4C). Similar results were seen by immunofluorescence for β -tubulin analysis of sections through the kidneys (Fig. 4B). Intriguingly, this increase in acetylation was largely observed in cystic epithelium.

Human polycystic kidney disease tissue also displays altered cytoplasmic microtubule PTMs

To determine if similar changes in microtubule PTMs are present in human ciliopathies, acetylated α -tubulin levels were determined in human polycystic kidney tissue. Autosomal recessive polycystic kidney disease (ARPKD; OMIM 263200) is a pediatric nephropathy with clinical features that include cyst formation in the renal collecting ducts, biliary dysgenesis, and portal tract fibrosis. ARPKD is caused by mutations in PKHD1 whose gene product Polyductin/Fibrocytin localizes to the cilium; however, ciliogenesis is not disrupted. Interestingly, in ARPKD human kidney samples (based on clinical findings and gross pathological examination) there is a large increase in the level of α -tubulin acetylation (Fig 4D). These data raise the possibility that signaling activities of the cilium and the cystic kidney disease proteins involve the entire microtubule network and reveal an unrecognized aspect of the consequences of cilia and cilia signaling disruption. Furthermore, these findings add to an emerging body of literature indicating that the cilium has an important function in regulating tubulin acetyltransferase enzymatic activity influencing the levels of cytosolic microtubule PTM.

Supplementary Material

Refer to Web version on PubMed Central for supplementary material.

Acknowledgments

We thank Yoder lab members for suggestions, Dr. Tamara Caspary (Emory University) for anti-Arl13b antibody; Dr. Carsten Janke (CNRS, France) for GT335 antibody. This work was funded by NIH RO1 DK065655 and DK075996 to BKY and a National Kidney Foundation fellowship to NS. NFB supported by NRSA 1F32DK088404. We acknowledge assistance from the UAB Hepatorenal Fibrocystic Kidney Disease Core Center (UAB RPKDCC, P30 DK074038).

References

- Akella JS, Wloga D, Kim J, Starostina NG, Lyons-Abbott S, Morrisette NS, Dougan ST, Kipreos ET, Gaertig J. MEC-17 is an alpha-tubulin acetyltransferase. *Nature*. 2010; 467(7312):218–22. [PubMed: 20829795]
- Bell PB Jr, Safiejko-Mroccka B. Improved methods for preserving macromolecular structures and visualizing them by fluorescence and scanning electron microscopy. *Scanning Microsc*. 1995; 9(3): 843–57. discussion 858–60. [PubMed: 7501997]
- Berbari NF, Johnson AD, Lewis JS, Askwith CC, Mykytyn K. Identification of ciliary localization sequences within the third intracellular loop of G protein-coupled receptors. *Mol Biol Cell*. 2008a; 19(4):1540–7. [PubMed: 18256283]
- Berbari NF, Kin NW, Sharma N, Michaud EJ, Kesterson RA, Yoder BK. Mutations in *Traf3ip1* reveal defects in ciliogenesis, embryonic development, and altered cell size regulation. *Dev Biol*. 2011; 360(1):66–76. [PubMed: 21945076]
- Berbari NF, Lewis JS, Bishop GA, Askwith CC, Mykytyn K. Bardet-Biedl syndrome proteins are required for the localization of G protein-coupled receptors to primary cilia. *Proc Natl Acad Sci U S A*. 2008b; 105(11):4242–6. [PubMed: 18334641]
- Blitzer AL, Panagis L, Gusella GL, Danias J, Mlodzik M, Iomini C. Primary cilia dynamics instruct tissue patterning and repair of corneal endothelium. *Proc Natl Acad Sci U S A*. 2011; 108(7):2819–24. [PubMed: 21285373]
- Davenport JR, Watts AJ, Roper VC, Croyle MJ, van Groen T, Wyss JM, Nagy TR, Kesterson RA, Yoder BK. Disruption of intraflagellar transport in adult mice leads to obesity and slow-onset cystic kidney disease. *Curr Biol*. 2007; 17(18):1586–94. [PubMed: 17825558]
- Ganguly A, Cabral F. New insights into mechanisms of resistance to microtubule inhibitors. *Biochim Biophys Acta*. 2011; 1816(2):164–71. [PubMed: 21741453]
- Goncalves A, Braguer D, Kamath K, Martello L, Briand C, Horwitz S, Wilson L, Jordan MA. Resistance to Taxol in lung cancer cells associated with increased microtubule dynamics. *Proc Natl Acad Sci U S A*. 2001; 98(20):11737–42. [PubMed: 11562465]
- Goold RG, Owen R, Gordon-Weeks PR. Glycogen synthase kinase 3beta phosphorylation of microtubule-associated protein 1B regulates the stability of microtubules in growth cones. *J Cell Sci*. 1999; 112 (Pt 19):3373–84. [PubMed: 10504342]
- Hammond JW, Huang CF, Kaech S, Jacobson C, Banker G, Verhey KJ. Posttranslational modifications of tubulin and the polarized transport of kinesin-1 in neurons. *Mol Biol Cell*. 2010; 21(4):572–83. [PubMed: 20032309]
- Haycraft CJ, Banizs B, Aydin-Son Y, Zhang Q, Michaud EJ, Yoder BK. *Gli2* and *gli3* localize to cilia and require the intraflagellar transport protein *polaris* for processing and function. *PLoS Genet*. 2005; 1(4):e53. [PubMed: 16254602]
- Hubbert C, Guardiola A, Shao R, Kawaguchi Y, Ito A, Nixon A, Yoshida M, Wang XF, Yao TP. HDAC6 is a microtubule-associated deacetylase. *Nature*. 2002; 417(6887):455–8. [PubMed: 12024216]
- Janke C, Bulinski JC. Post-translational regulation of the microtubule cytoskeleton: mechanisms and functions. *Nat Rev Mol Cell Biol*. 2011; 12(12):773–86. [PubMed: 22086369]
- Khawaja S, Gundersen GG, Bulinski JC. Enhanced stability of microtubules enriched in detyrosinated tubulin is not a direct function of detyrosination level. *J Cell Biol*. 1988; 106(1):141–9. [PubMed: 3276710]
- Konishi Y, Setou M. Tubulin tyrosination navigates the kinesin-1 motor domain to axons. *Nat Neurosci*. 2009; 12(5):559–67. [PubMed: 19377471]

- L'Hernault SW, Rosenbaum JL. Chlamydomonas alpha-tubulin is posttranslationally modified by acetylation on the epsilon-amino group of a lysine. *Biochemistry*. 1985; 24(2):473–8. [PubMed: 3919761]
- Loktev AV, Zhang Q, Beck JS, Searby CC, Scheetz TE, Bazan JF, Slusarski DC, Sheffield VC, Jackson PK, Nachury MV. A BBSome subunit links ciliogenesis, microtubule stability, and acetylation. *Dev Cell*. 2008; 15(6):854–65. [PubMed: 19081074]
- Mitchison T, Kirschner M. Dynamic instability of microtubule growth. *Nature*. 1984; 312(5991):237–42. [PubMed: 6504138]
- Piperno G, Fuller MT. Monoclonal antibodies specific for an acetylated form of alpha-tubulin recognize the antigen in cilia and flagella from a variety of organisms. *J Cell Biol*. 1985; 101(6):2085–94. [PubMed: 2415535]
- Quinones GB, Danowski BA, Devaraj A, Singh V, Ligon LA. The posttranslational modification of tubulin undergoes a switch from deetyrosination to acetylation as epithelial cells become polarized. *Mol Biol Cell*. 2011; 22(7):1045–57. [PubMed: 21307336]
- Sharma N, Bryant J, Wloga D, Donaldson R, Davis RC, Jerka-Dziadosz M, Gaertig J. Katanin regulates dynamics of microtubules and biogenesis of motile cilia. *J Cell Biol*. 2007; 178(6):1065–79. [PubMed: 17846175]
- Sharma N, Kosan ZA, Stallworth JE, Berbari NF, Yoder BK. Soluble levels of cytosolic tubulin regulate ciliary length control. *Mol Biol Cell*. 2011; 22(6):806–16. [PubMed: 21270438]
- Shida T, Cueva JG, Xu Z, Goodman MB, Nachury MV. The major alpha-tubulin K40 acetyltransferase alphaTAT1 promotes rapid ciliogenesis and efficient mechanosensation. *Proc Natl Acad Sci U S A*. 2010; 107(50):21517–22. [PubMed: 21068373]
- Wang Y, Veeraraghavan S, Cabral F. Intra-allelic suppression of a mutation that stabilizes microtubules and confers resistance to colcemid. *Biochemistry*. 2004; 43(28):8965–73. [PubMed: 15248754]
- Webster DR, Borisy GG. Microtubules are acetylated in domains that turn over slowly. *J Cell Sci*. 1989; 92 (Pt 1):57–65. [PubMed: 2674164]
- Yoder BK, Hou X, Guay-Woodford LM. The polycystic kidney disease proteins, polycystin-1, polycystin-2, polaris, and cystin, are co-localized in renal cilia. *J Am Soc Nephrol*. 2002; 13(10):2508–16. [PubMed: 12239239]
- Zhang Y, Li N, Caron C, Matthias G, Hess D, Khochbin S, Matthias P. HDAC-6 interacts with and deacetylates tubulin and microtubules in vivo. *Embo J*. 2003; 22(5):1168–79. [PubMed: 12606581]
- Zilberman Y, Ballestrem C, Carramusa L, Mazitschek R, Khochbin S, Bershadsky A. Regulation of microtubule dynamics by inhibition of the tubulin deacetylase HDAC6. *J Cell Sci*. 2009; 122(Pt 19):3531–41. [PubMed: 19737819]

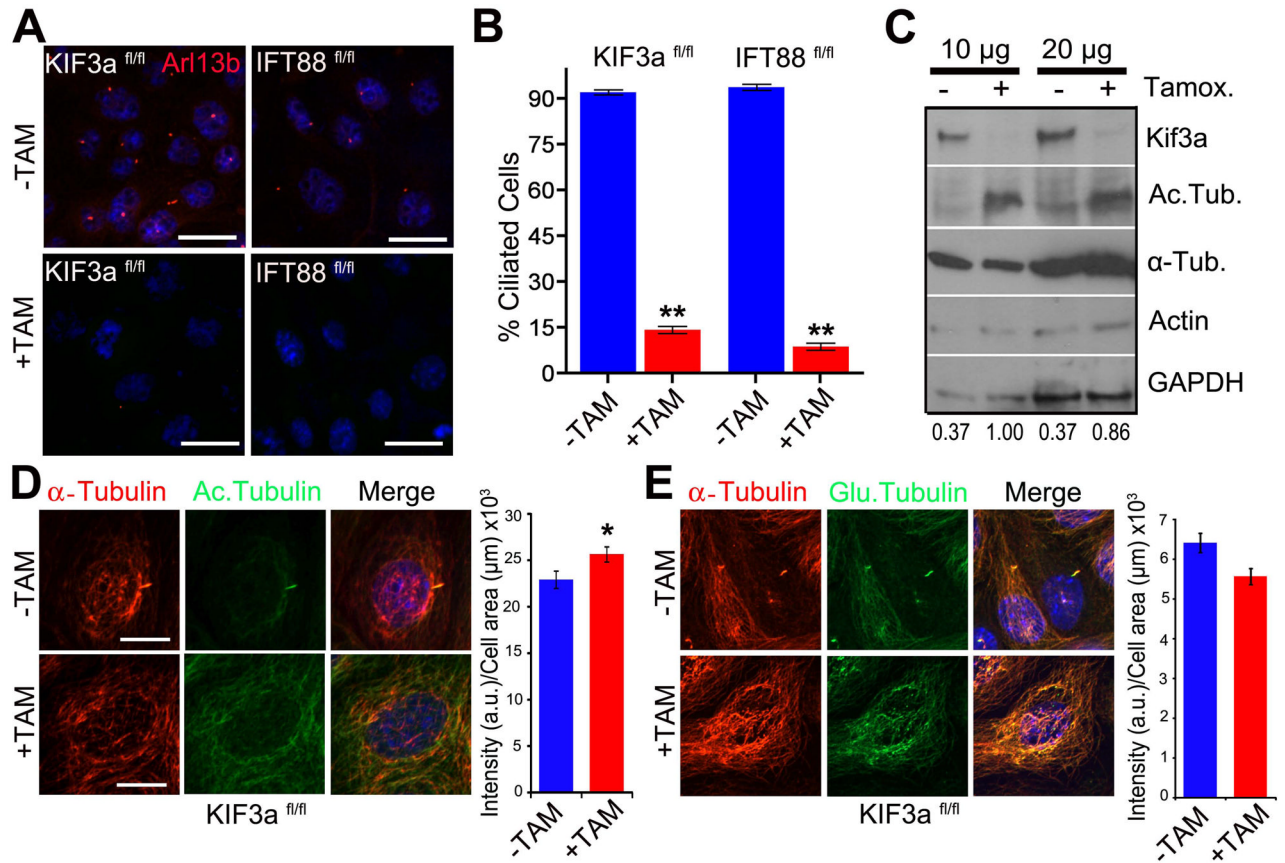


Figure 1. Loss of primary cilia is associated with increased α -tubulin acetylation

(A) Immunofluorescence staining for the cilia marker Arl13b (red) in wildtype noninduced (-TAM) and tamoxifen-induced (+TAM) *Kif3a*^{fl/fl}; CAAG-Cre^{ER} (*Kif3a*^{fl/fl}) and *IFT88*^{fl/fl}; CAAG-Cre^{ER} (*IFT88*^{fl/fl}) kidney epithelial cells. Scale bars 21 μ m. (B) Quantification of cilia in control (-Tam) and mutant (+Tam) *Kif3a*^{fl/fl} and *IFT88*^{fl/fl} cells. Bars show mean percent ciliated cells \pm SEM, asterisks indicate a significant change of measurements compared with the control group (Student's *t*-test; ***P* < 0.01). (C) Western blot analysis for α -tubulin acetylation, total α -tubulin, and actin using 10 μ g and 20 μ g of protein *Kif3a* mutant and control cells. Loading control is GAPDH. Numerical values at bottom are the densitometric ratio of acetylated α -tubulin to GAPDH normalized to the most intense band. (D, left panel) Immunofluorescence for α -tubulin (red) and acetylated- α -tubulin (green) in *Kif3a*^{fl/fl} conditional cells. Scale bar: 14 μ m. (D, right panel) A graph measuring the fluorescence intensity of acetylated α -tubulin staining comparing control (-TAM) and *Kif3a* mutant (+TAM) cells. Bars show mean acetylated tubulin intensity per μ m² of each cell \pm SEM, asterisks indicate a significant change of measurements compared with the control group (Student's *t*-test; **P* < 0.05). (E, left panel) Immunofluorescence for α -tubulin (α -tubulin, red) and poly-glutamylated tubulin (Glu. Tubulin, green) in *Kif3a*^{fl/fl} conditional mutant cells treated or nontreated with tamoxifen. Scale bar: 20 μ m. All nuclei stained with Hoechst in blue. (E, right panel) A graph measuring the fluorescence intensity of glutamylated α -tubulin staining comparing wildtype (-TAM) and cilia mutant (+TAM) cells. Bars show mean glutamylated tubulin intensity per μ m² of each cell \pm SEM (n=102,68; Student's *t*-test; *P* = 0.09)

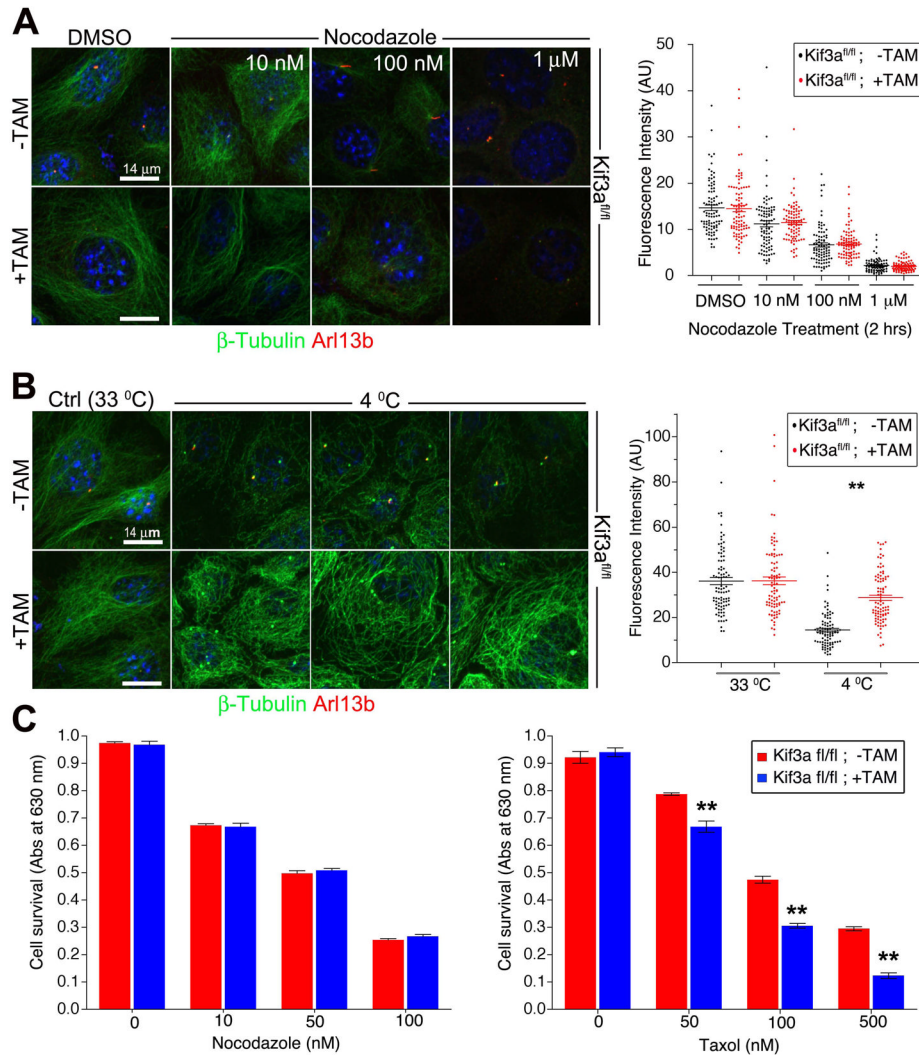


Figure 2. Microtubules in IFT/cilia mutants are more stable

(A) Immunofluorescence (left) analysis using cilia marker Arl13b (red) and β -tubulin (green) in ciliated (-TAM) and nonciliated (+TAM) *Kif3a* conditional cilia mutant cells treated with 10 nM, 100 nM and 1 μ M nocodazole or DMSO. Quantification (right) of the β -tubulin fluorescence intensity. Dot plots show arbitrary fluorescence intensities of cells from background subtracted images. Lines indicate the mean and SEM. Asterisks indicate a significant change of measurements compared with the control (DMSO) group (Student's *t*-test; ** $P < 0.01$) (B) Immunofluorescence (left) for Arl13b (red) and for β -tubulin (green) in ciliated (-TAM) and nonciliated (+TAM) *Kif3a* conditional mutant cells after exposure to 4°C or 33°C for 90 minutes. Quantification (right) of the β -tubulin fluorescence intensity. Dot plots show arbitrary fluorescence intensities of cells from background subtracted images, lines indicate the mean and SEM. Asterisks indicate a significant change of measurements compared with their corresponding control (-TAM) group (Student's *t*-test; ** $P < 0.01$) (C) Quantification of cell survival in ciliated (-TAM) and nonciliated (+TAM) cells after nocodazole (left) and Taxol (right) treatment. Bars show mean fraction of surviving cells \pm SEM. Asterisks indicate a significant change of measurements compared with the control group (Student's *t*-test; ** $P < 0.01$). Scale bars: 14 μ m. Nuclei stained with Hoechst are blue.

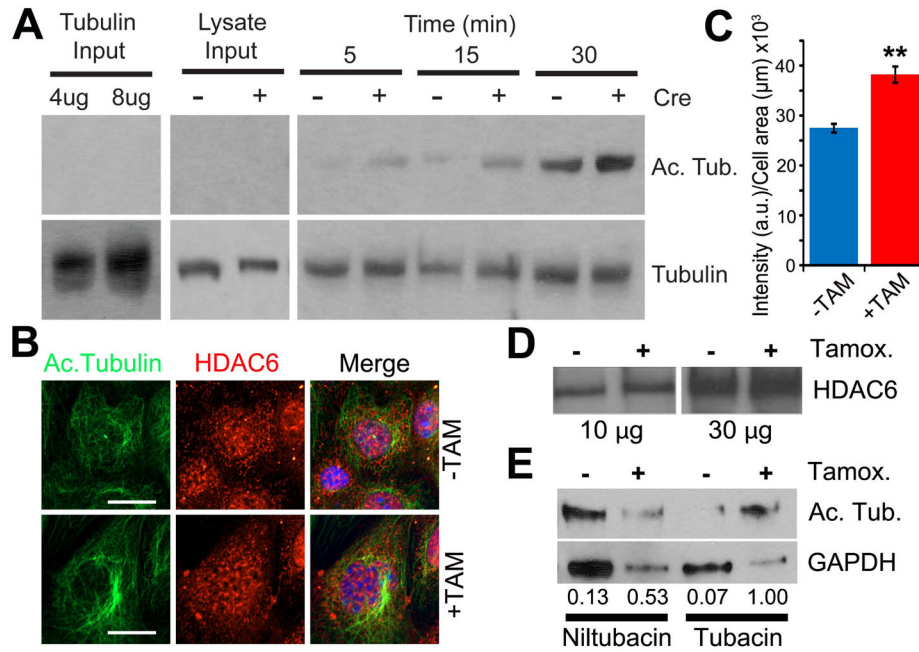


Figure 3. Increased microtubule acetylation activity in primary cilia mutant cells

(A) In vitro acetyl-transferase activity assay in cilia mutant and control cell extracts. Mec17 KO Tubulin substrate (Left panels, 4µg and 8µg of tubulin input alone) and 1µg of cell lysates from cilia mutants and controls (Middle panels, lysate inputs from Cre⁺ and Cre⁻ cells) were immunoblotted for both acetylated α-tubulin (Ac. Tubulin) and total α-tubulin (Tubulin). Tubulin acetylation reactions from cilia mutant and control cells (Cre⁺ and Cre⁻) were run for 5, 15 and 30 minutes (Right panels). (B) Immunofluorescence for acetylated α-tubulin and histone deacetylase 6 in cilia mutant and control cells (+TAM and -TAM). Hoechst stained nuclei in blue. Scale bars are 14µm. (C) A graph measuring the fluorescence intensity of HDAC6 staining comparing control (-TAM) and *Kif3a* mutant (+TAM) cells. Bars represent mean HDAC6 intensity per µm² of each cell ± SEM, asterisks indicate a significant change of measurements compared with the control group (Student's *t*-test; ***P* < 0.01). (D) Western blot analysis for HDAC6 expression in cilia mutant (Tamox. +) and control cells (Tamox. -) with 10 µg and 30 µg of total protein. (E) Western blot analysis for α-tubulin acetylation in *Kif3a* mutant and control cells treated with tubacin or niltubacin control. Loading control is GAPDH. Numerical values at bottom are the normalized densitometric ratio of acetylated α-tubulin to GAPDH

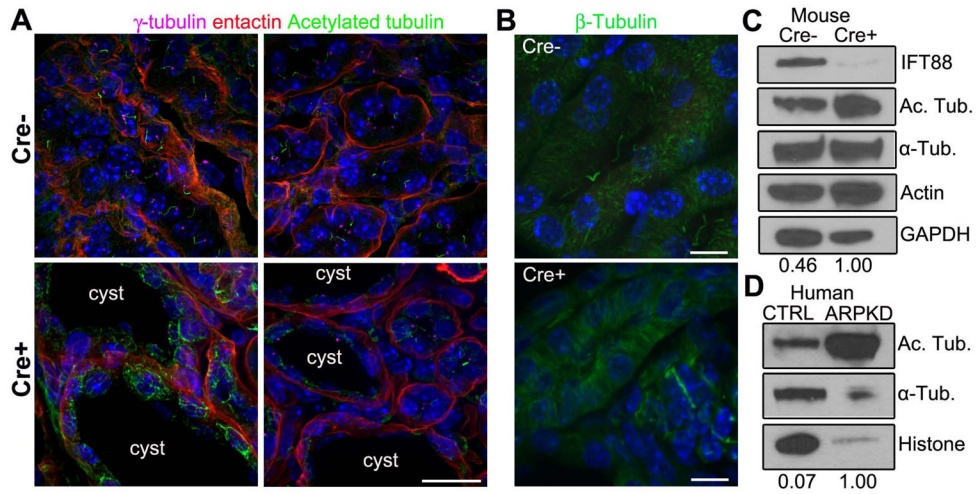


Figure 4. Increased α -tubulin acetylation in cilia mutant mouse tissue and human ARPKD cystic kidney disease patients

(A) Immunofluorescence for anti- γ -tubulin (purple), acetylated α -tubulin (green), and basement membrane marker entactin (red) in CAGG-CRE^{ER}; IFT88^{fl/fl} wildtype (Cre⁻) and cystic mutants (Cre⁺) kidneys. Scale bar 25 μ m. (B) Immunofluorescence analysis of the total microtubule network stained with β -tubulin (green) in cystic (Cre⁺) and non-cystic (Cre⁻) kidneys. All scale bars 15 μ m. Hoechst stained nuclei in blue. (C) Western blot analysis of ciliated (Cre⁻) and nonciliated (Cre⁺) kidneys probed for IFT88, acetylated α -tubulin, α -tubulin, actin and GAPDH. Numerical values at bottom are densitometric ratio of acetylated α -tubulin to GAPDH normalized to the most intense band. (D) Western blot analysis of control Control (CTRL) and ARPKD human samples probed for acetylated α -tubulin, α -tubulin and total histone, numerical values at bottom are normalized densitometric ratio of acetylated α -tubulin to histone.